Hydrogen – Hydrogen Bonding: A Stabilizing Interaction in Molecules and Crystals

Chérif F. Matta,[b] Jesús Hernández-Trujillo,[c] Ting-Hua Tang,[a] and Richard F. W. Bader*[a]

Abstract: Bond paths linking two bonded hydrogen atoms that bear identical or similar charges are found between the *ortho*-hydrogen atoms in planar biphenyl, between the hydrogen atoms bonded to the C1 – C4 carbon atoms in phenanthrene and other angular polybenzenoids, and between the methyl hydrogen atoms in the cyclobutadiene, tetrahedrane and indacene molecules corseted with tertiary-*tetra*-butyl groups. It is shown that each such H – H interaction, rather than denoting the presence of "nonbonded steric repulsions", makes a stabilizing contribution of up to 10 kcal mol^{-1} to the energy of the molecule in which it occurs. The quantum theory of atoms in molecules—the physics of an open system—demonstrates that while the approach of two bonded hydrogen atoms to a separation less than the sum of their van der Waals radii does result in an increase in the repulsive contributions to their energies, these changes are dominated by an increase in the magnitude of the attractive interaction of the protons with the electron density distribution, and the net result is a stabilizing change in the energy. The surface virial that determines the contribution to the total energy decrease resulting from the formation of the H – H interatomic surface is shown to account for the resulting stability. It is pointed out that H – H interactions must be ubiquitous, their stabilization energies contributing to the sublimation energies of hydrocarbon molecular crystals, as well as solid hydrogen. H – H bonding is shown to be distinct from "dihydrogen bonding", a form of hydrogen bonding with a hydridic hydrogen in the role of the base atom.

Keywords: bond path · density functional calculations · hydrogen bonds · hydrogen – hydrogen interaction

Introduction

Chemistry made evident in real space: Matter is a distribution of charge in real space, of pointlike nuclei embedded in the diffuse density of electronic charge, $\rho(\mathbf{r})$. All properties of matter are made manifest in the charge distribution, its topology delineating atoms and the bonding between them.[1] In a bound molecular state, the nuclei of bonded atoms are linked by a line along which the electron density is a maximum with respect to any neighboring line; they are linked by a *bond path*. The resulting *molecular graph*, that is, the linked network of bond paths that defines a system's molecular structure, has been shown to recover the structures in a multitude of systems, in terms of densities obtained from both theory[2, 3] and experiment,[4] structures that were previously inferred from classical models of bonding in conjunction with observed physical and chemical properties.

One correctly assumes that the physical presence of bonding between atoms denoted by the existence of a bond path, will also signify the presence of an accompanying energetic stabilization. This is indeed the case, as a bond path is mirrored by a *virial path* linking the same nuclei, along which the potential energy density is maximally stabilizing.[5] Thus co-existing with every molecular graph, is a shadow graph—the virial graph—indicating the presence of a corresponding set of lines, again defined in real space, that delineates the lowering in energy associated with the formation of the structure defined by the molecular graph. Chemistry is observation: of charge distributions, of geometries, of energy changes, and of the emission and absorption of electromagnetic radiation. Bonding, like other properties, should be evident in the measurable properties of a

[a] Prof. R. F. W. Bader, Dr. T.-H. Tang
Department of Chemistry, McMaster University
Hamilton Ont. L8S 4M1 (Canada)
Fax: (1) 905-522-2509
E-mail: bader@mcmaster.ca

[b] Dr. C. F. Matta
Lash Miller Chemical Laboratories
Chemistry Department, University of Toronto
Toronto Ont. M5S 3H6 (Canada)

[c] Dr. J. Hernández-Trujillo
Departamento de Fisica y Quimica Teórica
Facultad de Quimica
Universidad Nacional Autónoma de México
México D. F. 04510 (México)

DOI: 10.1002/chem.200204626

system. The quantum theory of atoms in molecules (QTAIM) is quantum mechanics applied to a system's measurable charge distribution and it provides the atomic basis for all measurable properties.[6]

There are many systems in which the bonding is between closed-shell systems, and the classical models used to assign a bonded structure based on the Lewis electron-pair model or its analogue expressed in terms of the overlap of suitably occupied atomic orbitals is not applicable. Hydrogen bonding together with the bonding in molecular crystals and ionic solids are examples of closed-shell interactions. The topology of the density and the physics that determines it, however, transcend all models, and the presence of a bond path linking the nuclei of a pair of atoms in any of these structures unequivocally identifies them as being bonded to one another.[7] The directed intermolecular bond paths observed in the experimental charge distribution of solid chlorine, for example, account for its layered structure, a structure inexplicable in terms of van der Waals forces or "nonbonded interactions".[8]

The bond path provides an operational definition of chemical bonding, one that can be directly related to experimental observation. Many examples of bond paths indicating the presence of intermolecular bonding have been observed in experimental crystal densities. Koritsanszky and Coppens,[4] in a review of applications of the topological analysis to high-resolution X-ray densities, comment on the ability of the theory to identify and define atomic connectivities that lie beyond the scope of classical models. Flaig et al.[9] report a bond critical point analysis of inter- and intramolecular bonding, including strong to weak hydrogen bonds, defined within the experimental charge densities of amino acids. Espinosa, Molins, and Lecomte[10] have analyzed the topological properties of the density obtained from accurate X-ray diffraction experiments for 83 structures possessing an X–H···O link and have shown that energy quantities modeled on the density and its Laplacian at the bond critical point exhibit a universal relationship with the H–O distance. Two recent reviews of applications of QTAIM[11, 12] contain discussions of and references to the many recent topological analyses of experimentally determined charge distributions, for both inter- and intramolecular interactions. Included is a description of the work identifying a Mn-H-H-C dihydrogen bond path in the experimental charge density of a Mn complex.[13]

The present paper considers closed-shell hydrogen–hydrogen (H–H) interactions, wherein a bond path links a pair of identical or similar hydrogen atoms that are close to electrical neutrality, that is, interactions that fall within the classical category of nonbonded or van der Waals interactions. Such interactions are found to link hydrogen atoms bonded to both unsaturated and saturated carbon atoms in hydrocarbon molecules, as illustrated in Figures 1 and 2 for the systems under study here. It is demonstrated that H–H interactions contribute a stabilizing contribution to the energy, even in cases considered to involve "steric nonbonded repulsions"[14] resulting from the approach of two hydrogen atoms to within their van der Waals radii as found, for example, in planar biphenyl.

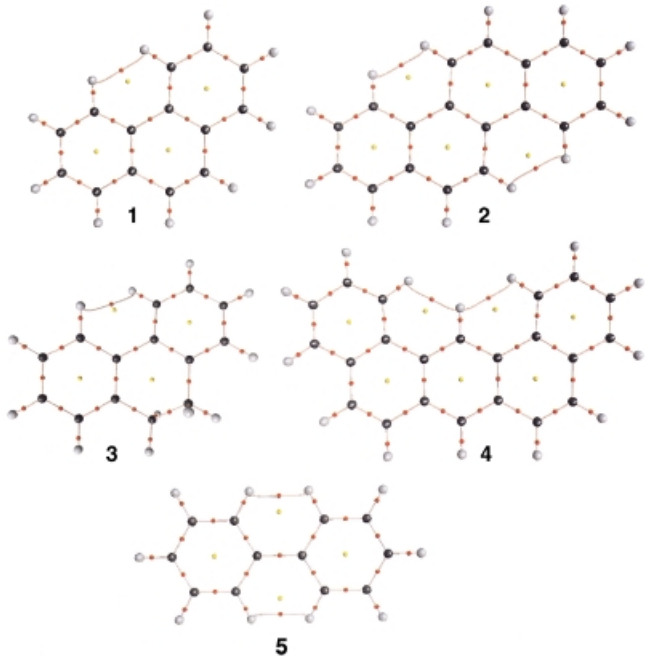

Figure 1. Molecular graphs for phenanthrene (**1**), chrysene (**2**), 9,10-dihydrophenanthrene (**3**), dibenz[a,j]anthracene (**4**), and planar biphenyl (**5**). Bond critical points (CPs) are red, ring CPs yellow. Note the close proximity of the bond and ring CPs for the H–H bonded ring in **3** and the very curved nature of the H–H bond path for the 6–31G** basis set.

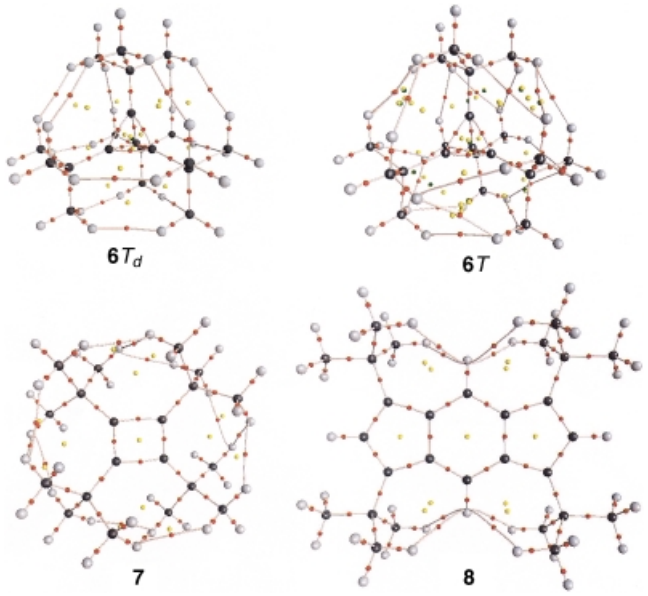

Figure 2. Molecular graphs for the T_d and T structures of tetra-*tert*-butyltetrahedrane (**6**), tetra-*tert*-butylcyclobutadiene (**7**) and tetra-*tert*-butylindacene (**8**). Bond CPs are in red, ring CPs in yellow. Note how the H–H bond paths linking the methyl hydrogens in **6** and **7** effectively encapsulate the otherwise unstable central cage and ring structures of four carbon atoms. Correspondingly, the eight H–H bond paths in **8** stabilize its D_{2h} structure. Note the proximity of the bond and ring CPs associated with the bifurcated rings in **6** *T*, for the 6–31G** basis set.

The H–H interaction existing between identically or similarly charged hydrogen atoms is to be sharply distinguished from what is termed a "dihydrogen bond", one dominated by the electrostatic interaction between two

hydrogens of opposite charge. A dihydrogen bond is a particular kind of hydrogen bond whereby the role of the base atom B in A-H-B is assumed by a hydridic hydrogen. There is a considerable amount of literature on dihydrogen bonding with a recent review by Custelcean and Jackson.[15] The field begins with the classic example of the hydrogen bonding resulting in the dimerization of BH_3NH_3.[16] Since dihydrogen bonding is dominated by electrostatic contributions, its formation is restricted to systems that possess a hydridic hydrogen, such as one bonded to a transition metal or to a metal from Groups 1, 2, and 3. Popelier, for example,[17] in a study of the dimer of BH_3NH_3, finds the hydridic H atom bound to boron and the acidic H atom bound to nitrogen to bear charges of -0.7 and $+0.5$ e, respectively. Popelier demonstrated that the dihydrogen bonding in this dimer exhibits the characteristics of hydrogen bonding, as determined by the electron density and atomic properties within the framework of QTAIM. Grabowski[18–21] has conducted an extensive theoretical study of the geometries and energetics of dihydrogen bonding and has employed bond critical point properties in an analysis of these interactions. He finds, for example, that an MP2 calculation with a large basis set yields a dihydrogen bond energy of 12.6 kcal mol^{-1} for the complex F-H-H-Li, in which the hydrogen atoms in the free LiH and HF molecules bear net charges of -0.9 e and $+0.7$ e, respectively. Kulkarni and Srivastava[22] studied dihydrogen bonding of LiH, BH_3, and AlH_3 with third-row hydrides, contrasting their properties with the second-row congeners. Weak dihydrogen bonds between a methyl hydrogen atom and a hydrogen atom of an amino group are found in four rotamers of the amino acid leucine.[23] Recently Del Bene et al.[24] published an in-depth theoretical study of a range of dihydrogen complexes from strong to weak, with emphasis on a comparison of calculated and experimental properties. A bond critical point analysis was employed in all of these studies. The analysis presented here will contrast H–H bonding with dihydrogen bonding, showing that the two differ in both their geometrical and energetic characteristics, representing two extremes of possible interactions between hydrogen atoms.

The underlying physics: Among the most important results obtained from the quantum theory of atoms in molecules is its demonstration of the intimate relationship that exists between the distribution of the electron density within an atomic basin and the atom's contribution to a molecule's properties. The reason for this is readily understood. Any two pieces of matter, including two atoms, are identical and possess identical properties only if they possess identical charge distributions, that is, they are indistinguishable in real space. Since an atom of theory is defined by its charge distribution as a bounded region of real space, its form necessarily reflects its properties. The physics of an atom in a molecule[6]—the physics of an open system—defines every measurable property expressed as an expectation value of a Hermitian operator, in terms of a corresponding "dressed" density distribution, one whose integration over an atomic basin yields the atom's additive contribution to that property.[25] A dressed density distribution for some particular property accounts for the corresponding interaction of the density at some point in space with the remainder of the molecule, and it exhibits the same degree of atomic transferability between molecules as does the electron density.

A dressed density distribution of particular importance is the virial field $V(\mathbf{r})$, which represents the energy of interaction of an electron at some position $\mathbf{r}$ with all of the other particles in the system, averaged over the motions of the remaining electrons.[1] When integrated over all space it yields the total potential energy of the molecule, including the nuclear energy of repulsion, and for a system in electrostatic equilibrium, it equals twice the molecule's total energy. The virial field condenses all of the electron–electron, electron–nuclear, and nuclear–nuclear interactions, described by the many-particle wave function, into an energy density that is distributed in real space. Not only does the virial field, which is everywhere negative, mimic the transferability of the density and thus account for the existence of experimental additivity schemes for heats of formation, its magnitude $|V(\mathbf{r})|$ is structurally homeomorphic with the electron density; that is, every structure and change in structure exhibited in the topology of $\rho(\mathbf{r})$ is recovered in the topology of $|V(\mathbf{r})|$, and it is this topology that defines the virial path discussed above.[5] This congruence in the topological features of the electron density distribution and the lowering of the energy is made clear in a comparison of molecular graphs in Figures 1 and 2, with the corresponding virial graphs in Figure 3. A bond path in a molecular graph is mirrored by a virial path in the virial graph, showing that each bonding line of maximum electron density generates a virial line of minimum potential energy.

It is important to realize that no *net* force acts on any of the nuclei nor on the electrons in an equilibrium geometry of a molecule in a bound state. Nuclear forces do arise as a result of the ever present nuclear excursions about the equilibrium configuration, but these are directed so as to return the system to its equilibrium geometry. The variational principle ensures that every wave function and its derived density distribution minimize the system's total energy, and the network of bond paths is the result of the system's charge distribution responding so as to minimize the total energy for a given nuclear configuration.

H–H bonding: The molecular graphs of the hydrocarbon molecules studied here, **1** to **8**, are illustrated in Figures 1 and 2. Bond paths are found between the pairs of hydrogens linked to 1,4-carbon atoms in planar, unsaturated hydrocarbons: as found in the "bay regions" of phenanthrene (**1**) and chrysene (**2**), and in twisted 9,10-dihydrophenanthrene (**3**). The unique hydrogen extended into the enlarged bay region of dibenz[a,j]anthracene (**4**), participates in bifurcated H–H bonding. Two H–H interactions are found in the planar structure of biphenyl (**5**). The *tert*-butyl group is used to stabilize molecules whose parent structures are thermodynamically unstable, by effectively enclosing the parent structure in a box that can be opened only by forcing the hydrogen atoms of the *tert*-butyl methyl groups into closer contact, termed the "corset effect" by Maier.[26] Examples of such structures are the tetra-*tert*-butyl derivatives of the

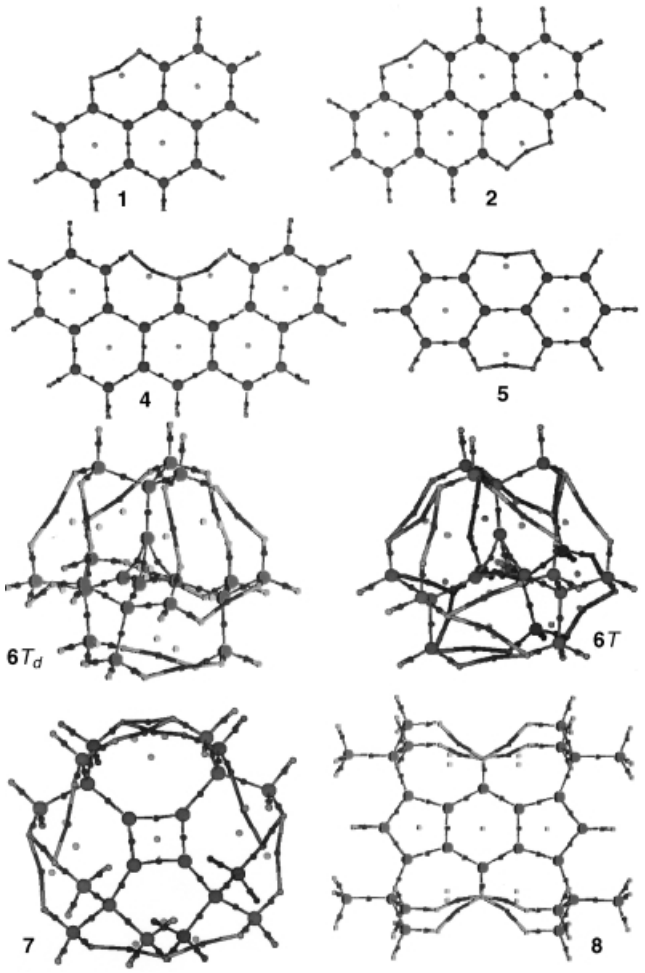

Figure 3. Virial graphs for phenanthrene (**1**), chrysene (**2**), dibenz[a,j]anthracene (**4**), planar biphenyl (**5**), the T_d structure of tetra-*tert*-butyltetrahedrane (**6**), tetra-*tert*-butylcyclobutadiene (**7**), and tetra-*tert*-butylindacene (**8**) for the 6 – 31G** basis set and for the *T* structure of tetra-*tert*-butyl tetrahedrane for the 6 – 311 ++ G(2d,1p) basis set. Note that the separations between the bond and ring CPs for the H – H interactions in the virial field are generally smaller than in they are in $\rho(\mathbf{r})$, and their coalesence will, in general, occur at longer H – H separations, a separation longer than the equilibrium value of R(H – H) found for 9,10-dihydrophenanthrene (**3**).

structural isomers of C_4H_4, tetra-*tert*-butyltetrahedrane (**6**)[27] and tetra-*tert*-butylcyclobutadiene (**7**). The outer cage enclosing these molecules is uniquely defined by the network of bond paths that link the hydrogen atoms of the methyl groups of neighboring *tert*-butyl groups. This paper will demonstrate that the stability of these molecules is partially accounted for in terms of the energy required to disrupt the encasing network of H – H bond paths that number 18 in **6** and 12 in **7**. The final related example is 1,3,5,7-tetra-*tert*-butyl-*s*-indacene (**8**), whose D_{2h} structure has been confirmed by a low-temperature X-ray diffraction experiment on its crystalline form.[28] The electron density distribution of this molecule has recently been determined in an accurate X-ray diffraction experiment.[29] The experimental density indicates the presence of bond paths linking each of the apical hydrogen atoms of the benzene ring to four hydrogen atoms of four separate methyl groups, to yield a structure with eight H – H bonded interactions; a result in accord with the theoretical molecular graph, Figure 2. The linear isomers of **1** and **2**, anthracene and tetracene, respectively, are also investigated to determine properties of hydrogen atoms in related systems that do not exhibit H – H bonding

The bond paths linking 1,4-carbon atoms in the molecules **1**, **2**, and **5** have been previously reported and studied by Cioslowsky and Mixon.[14] The two H – H bond paths linking 1,4-carbon atoms in the planar geometry of biphenyl, $\phi = 0^\circ$, yield two six-membered rings and two corresponding ring critical points (CPs). An increase in ϕ from 0 to 27° causes each of the H – H bond paths to vanish, as a result of the coalescing of each of the bond CPs with the associated ring CP in a fold catastrophe; Cioslowsky and Mixon used the equation for such a catastrophe to relate the dependence of the bond and ring CP properties on the interproton separation R(H – H). Their critical value of 2.18 Å, above which they state no H – H interaction line should appear, is exceeded in the bond paths encountered between methyl hydrogen atoms of the *tert*-butyl groups forming the cage structures in **6**, **7**, and **8**.

Because of their presence in systems in which R(H – H) is less than the sum of the van der Waals radii, Cioslowski and Mixon, following the classical interpretation of a "nonbonded steric interaction", concluded that the H – H interaction lines in these molecule denoted repulsive rather than bonded interactions between the hydrogen atoms. There are no forces, attractive or repulsive, operative in these molecules at the geometries under discussion, and it will be shown that the formation of the H – H interactions lines in these molecules lead to a lowering of the energy of the systems in which they are found and that the H – H interactions satisfy all requirements of bonding.

Computational Methods

Molecular energies and electron densities were obtained in B3LYP 6-31G**//B3LYP 6-31G** calculations using Gaussian 94 for all of the molecules.[30] Atomic and bond CP properties were obtained using AIMPAC;[31] the molecular and virial graphs were calculated and plotted using AIM2000.[32, 33] The atomic energies for the equilibrium geometries were obtained from the atomic statement of the virial theorem that relates the total energy $E(\Omega)$ of atom Ω to its electronic kinetic energy $T(\Omega)$ through the relationship $E(\Omega) = -T(\Omega)$. The equivalent statement of the molecular virial theorem, which requires that the ratio $\gamma = -V/T$ equal 2, was, in general, not exactly satisfied. To correct for this, each $T(\Omega)$ was multiplied by the factor $-(\gamma - 1)$ rather than -1 to obtain $E(\Omega)$. The value of γ for the large hydrocarbons studied here can deviate from 2 by as much as 0.01. While the corrections do scale linearly with respect to $T(\Omega)$, being smallest for the H atoms and leaving the relative stabilities of the atoms unchanged, we also performed self-consistent virial scaling (SCVS) calculations for biphenyl in its planar and equilibrium geometries and for the phenanthrene/anthracene pair of molecules at the restricted Hartree – Fock (RHF) level of theory using the 6-31G** basis set. These were SCF calculations wherein the electronic coordinates were scaled so as to satisfy the virial theorem, the deviation in γ from its correct value of 2 being reduced to 1×10^{-9}, while simultaneously re-optimizing the geometry. The SCVS results demonstrated that the relative stabilities of the atoms do not change when the virial theorem is satisfied and that the correction term of $-(\gamma - 1)$ correctly predicts the relative atomic stabilities in these systems, as it has been found to do in others.

Optimized RHF wave functions for the planar geometry and the twisted equilibrium geometry of biphenyl were also obtained using the 6-311 ++

G(2d,2p) basis set, and additional MP2 6-31G**//MP2 6-31G** calculations were carried out for the phenanthrene/anthracene pair. The calculations demonstrated that the relative ordering of the atomic energies remain unaltered by the SCVS procedure, by an increase in basis set, or by the addition of electron correlation. Because of the weak nature of the H–H interactions between the methyl hydrogens in **6** and **7**, wave functions and densities for these molecules were also calculated by using the larger 6-311++G(2d,2p) basis set in B3LYP calculations at the previously determined 6-31G* geometry.[34] The calculated molecular graphs and in particular the presence of the H–H bond paths were invariant to the choice of basis set and level of theory for all of the molecules.

Results and Discussion

Properties of the bond critical points: Table 1 presents the values of the internuclear separation R(H–H), under the heading BL, and the bond critical point (CP) data for the bonded H–H interactions in the molecules **1** to **8** shown in Figures 1 and 2. All results are obtained from the B3LYP/6-31G** calculations. The changes in these values with basis set and level of theory are too small to be of physical significance. While the values of R(H–H) for the hydrogen atoms bonded to 1,4-carbon atoms in the unsaturated systems are all less than 4.0 au, a value less than twice the van der Waals radius of hydrogen equal to 4.5 au, the H–H separations found between the H atoms bonded to the saturated carbons of the methyl groups in **6**, **7**, and **8**, all exceed 4.1 au and are found to occur at a separation as large as 5.1 au in **6**. The bond paths for all of the H–H interactions are curved with the bond path length (BPL), exceeding the bond length by as much as 0.5 au (Table 1). As anticipated, the H–H interactions exhibit the characteristics of closed-shell interactions: a low value for the density at the bond CP (ρ_b), relatively small corresponding positive values for the Laplacian ($\nabla^2\rho_b$), and a positive value for the energy density H_b that is close to zero. The values of ρ_b decrease in a nearly linear fashion with increasing H–H internuclear separation. The experimental and calculated values of ρ_b for **8** are in good agreement.

While the values of the bond CP indices are typical of those found for weak hydrogen bonds, being somewhat larger in value than those for van der Waals interactions,[35] it is important to note the features that distinguish H–H bonding from dihydrogen bonding, aside from and in addition to the evident feature that both hydrogens in the H–H interaction exhibit identical or similar properties. The energy density H_b becomes negative for strong hydrogen bonds and correspondingly, for strong dihydrogen bonds. It is demonstrated below that the energy of each of the hydrogen atoms forming the H–H link can decrease by as much as 6 kcal mol^{-1}; this places the H–H interaction well outside the range of van der Waals interactions and weak hydrogen bonds and within the range of moderately strong hydrogen bonded systems. Nonetheless, the kinetic energy density at the bond CP (G_b) dominates the potential energy density (V_b) for all the H–H interactions, and H_b remains small and positive.

There is a more striking distinction to be made between H–H bonding and dihydrogen bonding. One of the most characteristic features of hydrogen bonding is the increase in the length of the A–H bond in A-H-B, and a concomitant red shift in its vibrational frequency, a feature that persists for the A–H participant in dihydrogen bonding.[24] In H–H bonding on the other hand, the lengths of the C–H bonds linked by the H–H bond path both undergo a significant *decrease* in length of 0.002–0.004 Å. Further important differences in the physics underlying H–H and dihydrogen bonding are made clear in the comparison of the atomic properties given below.

The presence of an intramolecular H–H bond path necessitates the formation of a ring structure and an associated ring critical point. The breaking of the H–H bond path requires that the bond and ring CPs coalesce upon attaining a common value, as described above in the twisting of the rings in biphenyl. The approach of the two CPs causes the negative curvature of the density at the bond CP lying along the axis of their approach and the associated positive curvature of the ring CP to approach zero; the vanishing of the curvatures upon coalesence indicating the formation of an unstable CP. Thus the ellipticity (ε) at the bond CP—determined by the ratio of the largest to the smallest of the magnitudes of the two negative curvatures—becomes infinitely large immediately preceding the coalescence of the CPs. Figures 1 and 2 indicate the positions of both the bond and ring critical points and their separations are given in Table 1. With the exceptions of 9,10-dihydrophenanthrene (**3**) and the ring structure

Table 1. Bond critical point data in atomic units and stabilization energies in kcal mol^{-1} for H–H bonding.

Molecule	ρ_b	ρ_r	$\mathbf{r}_b - \mathbf{r}_r$	$\nabla^2\rho_b$	ε	G_b	V_b	H_b	BL	BPL	E(H–H)
1	0.0120	0.0107	0.895	0.0485	0.498	0.0095	–0.0069	0.0026	3.804	4.046	9.4
2	0.0133	0.0114	0.974	0.0528	0.435	0.0106	–0.0080	0.0026	3.707	3.932	11.2
3	0.0102	0.0100	0.620	0.0443	1.208	0.0083	–0.0055	0.0028	4.057	4.571	3.1
4	0.0126	0.0110	0.921	0.0501	0.457	0.0100	–0.0075	0.0025	3.757	3.982	10.0
5	0.0136	0.0114	1.010	0.0535	0.403	0.0108	–0.0083	0.0026	3.686	3.900	10.4
6 (*Td*)	0.0065	0.0036	1.577	0.0218	0.060	0.0043	–0.0031	0.0012	4.247	4.284	1.6
6 (*T*)	0.0048	0.0034	1.358	0.0163	0.062	0.0031	–0.0021	0.0010	4.587	4.670	0.8
	0.0028	0.0027	0.681	0.0093	0.103	0.0017	–0.0011	0.0006	5.133	5.233	
7	0.0168	0.0055	1.871	0.0513	0.021	0.0121	–0.0114	0.0007	3.413	3.457	4.6
	0.0152	0.0052	1.944	0.0479	0.010	0.0110	–0.0100	0.0010	3.511	3.557	
	0.0068	0.0055	1.140	0.0251	0.356	0.0048	–0.0034	0.0015	4.373	4.547	
	0.0080	0.0057	1.309	0.0296	0.285	0.0058	–0.0041	0.0016	4.196	4.339	
8	0.0081	0.0064	1.247	0.0307	0.267	0.0059	–0.0042	0.0018	4.161	4.161	3.8[a]
exptl. values[29]	0.0083			0.0336	0.590						

[a] For two of the four H–H interactions linked to one benzenoid H atom.

associated with the bifurcated H – H bonding in the *T* structure of **6**, significant separations ($\mathbf{r}_b - \mathbf{r}_r$) are seen to exist between the bond and ring CPs, with values in excess of 0.9 au. In addition, significant differences exist between the values of the density at the bond and ring (ρ_r) CPs with the same two exceptions (Table 1). Correspondingly, their bond ellipticities are all less than 0.5, and the structures are stable with respect to displacements of the nuclei. In **3** however, the ellipticity equals 1.2, the two CPs are separated by 0.6 au, and their densities differ in value by only 2×10^{-4} au. A small increase in the dihedral angle between the two aromatic rings, from its equilibrium value of $\sim 23^{\circ}$, results in the coalescence of the two CPs and in the breaking of the H – H bond path. The H – H interaction in this molecule has the lowest value for ρ_b in the benzenoids and is closest to instability. The subsequent analysis will show that it is energetically the weakest of the benzenoid H – H interactions in this study. The longest and weakest H – H bonds in the series are those associated with the bifurcated bonding in the *T* structure of **6** with $\rho_b = 0.0028$ au, differing from ρ_r by only 1×10^{-4} au. While the associated ellipticity is not large, this is a result of all of the associated curvatures being of small magnitude, ~ 0.001 au. The instability of the H – H interactions in **6***T* and in **3** are reflected in the absence of the associated virial paths; the associated bond and ring CPs of the virial field having already coalesced at the equilibrium geometries. However, *all* the virial paths are present in **6***T* from the results for the larger 6-311 ++ G(2d,2p) basis set. The H – H interactions in biphenyl are present in the planar structure, transitional between the two equivalent twisted equilibrium geometries. They will be formed and broken by the zero-point internal rotation about the C – C axis linking the two rings surmounting the 2 kcal mol^{-1} barrier.

The polybenzenoids (1, 2, 3, and 4): The bond paths present in the bay regions of phenanthrene (**1**) and chrysene (**2**) are normally classed as examples of "nonbonded steric repulsive interactions", when in fact the heats of formation of both **1** and **2** are ~ 6 kcal mol^{-1} less than those of their respective linear isomers, anthracene and tetracene.[36] The RHF calculations predict **2** to be more stable than tetracene by 10.2 kcal mol^{-1} and **1** to be more stable than anthracene by 5.1 kcal mol^{-1}, a value that increases to 6.4 kcal mol^{-1} for the MP2 calculation and to 6.9 kcal mol^{-1} for the SCVS calculation.

There is a transfer of electronic charge from the carbon atoms to the hydrogen atoms when the linear benzenoids anthracene and tetracene are transformed into their isomeric forms **1** and **2**, 0.0093 e in **1** and 0.0169 e in **2**. Consequently, the carbon atoms are most stable in the linear isomers, with the carbon atoms in anthracene being more stable by 8.0 kcal mol^{-1} and those in tetracene by 16.5 kcal mol^{-1}. Thus the extra stability of **1** and **2** over their linear analogues resides in the hydrogen atoms. The hydrogen atoms in **1** are more stable by 12.1 kcal mol^{-1} and those in **2** by 26.1 kcal mol^{-1} than in the linear isomers. While the energies of the hydrogen atoms in the linear analogues exhibit a spread of only 0.2 kcal mol^{-1}, this is not the case for **1** and **2** in which the hydrogen atoms that participate in H – H bonding show a marked increase in their stability relative to the those in the linear isomers; 4.7 kcal mol^{-1} per hydrogen in **1** and 5.6 kcal mol^{-1} per hydrogen in **2**. Each of the remaining eight hydrogen atoms, termed *normal hydrogen atoms*, are similarly stabilized by 0.3 kcal mol^{-1} in **1** and by 0.5 kcal mol^{-1} in **2**. Thus the H – H bonded interaction contributes $2 \times 4.7 =$ 9.4 kcal mol^{-1} to the excess stability of **1**, and each such H – H interaction contributes 11.2 kcal mol^{-1} to the excess stability of **2**. The same analysis from the results of the RHF-SCVS calculation for phenanthrene yields a stabilization of 12.8 kcal mol^{-1} for the H – H interaction, the remaining hydrogen atoms being stabilized by 0.4 kcal mol^{-1} relative to those in anthracene. In an analogous manner, the MP2 calculation yields a stabilization of 10.0 kcal mol^{-1} for the H – H interaction in phenanthrene, a value closer to the B3LYP result of 9.4 kcal mol^{-1} than to the RHF SCVS results. We define the H – H stabilization energy E(H – H) to be the energy lowering associated with the hydrogen atoms involved in H – H bonding. Whether the energy lowering is gauged relative to the energies of the other normal hydrogen atoms in the same molecule or to those in a related molecule, the value of E(H – H) changes by less than 1 kcal mol^{-1}. The values of E(H – H) are given in Table 1.

No isomers without H – H bonds of the molecules of 9,10-dihydrophenanthrene (**3**) and dibenz[a,j]anthracene (**4**) were considered, isomers that would provide a standard for the determination of the increased stability of the H – H bonded hydrogen atoms. However, the average energies of normal benzenoid hydrogen atoms exhibit only small variations in all these molecules, and one can obtain a measure of the increased stability resulting from the presence of H – H bonding in **3** and **4** by comparing the energies of the H – H bonded hydrogen atoms in these molecules with the same standard energies used in the determination of the H – H bonding energy in **1** and **2**. This procedure yields a result of 3.1 kcal mol^{-1} for E(H – H) in **3**, a value approximately one-third as large as that found for **1**. This result is not unexpected in light of the close proximity of the bond and ring CPs for this interaction (Figure 1), a proximity that reduces the value of ρ_b and places the interaction on the verge of annihilation.

The stability resulting from the presence of two H – H interactions in chrysene is approximately twice that resulting from the single such interaction in phenanthrene. This approximate additivity of E(H – H) carries over to the bifurcated H – H bonding found in dibenz[a,j]anthracene (**4**). In this molecule, the excess stability of 9.5 kcal mol^{-1} found for the central hydrogen atom that serves as the terminus for two H – H bond paths equals twice the value for a H – H bonded hydrogen atom in phenanthrene, while each hydrogen atom bonded to the bifurcated hydrogen atom in **4** is stabilized by 5.2 kcal mol^{-1}. Thus each H – H interaction contributes a stabilizing contribution of 10.0 kcal mol^{-1} to the energy of **4**.

The stabilization of a hydrogen atom bonded to an aromatic ring that is involved in H – H bonding is calculated to be approximately 5 kcal mol^{-1} in phenanthrene, chrysene, and dibenz[a,j]anthracene. Thus the presence of hydrogen atoms with a separation of less than 4 au in these molecules does not result in "a repulsive steric interaction", but rather in the

formation of a bond path and a stabilizing contribution to the energy, as anticipated for a bonded interaction. The stabilization overrides the accompanying decrease in the stability of the carbon framework in phenanthrene and chrysene, and the presence of the H – H bonding imparts an increased stability to these molecules over their linear isomers. There is no attempt to define a corresponding "H – H bond energy". The energy changes associated with the presence or absence of H – H bonding are not restricted to the hydrogen atoms involved in the bonding, and one is faced with the usual ambiguities in attempting to define a "bond energy" in such cases. What one can unambiguously define is the H – H stabilization energy E(H – H), the contribution to the lowering of the energy of the entire molecule that resides in the energy associated with the hydrogens involved in H – H bonding.

Biphenyl (5): The calculated B3LYP 6-31G** twisted equilibrium geometry of biphenyl ($\phi = 38^{o}$) is calculated to lie 2.1 kcal mol^{-1} lower in energy than the planar geometry ($\phi = 0^{o}$) and 2.5 kcal mol^{-1} lower in energy than the perpendicular geometry ($\phi = 90^{o}$). This energy ordering is in agreement with experiment, which places the two barriers at 1.4 and 1.6 kcal mol^{-1} and the equilibrium value at $\phi = 44.4^{o}$.[37] The RHF SCVS 6-31G** calculation gives $\phi = 45.5^{o}$ and the RHF with the large basis set gives $\phi = 46.5^{o}$. The classical arguments for these observations are that the perpendicular geometry breaks the delocalization of the π density over the two rings, while the planar structure is subject to "steric nonbonded repulsion". The attainment of the planar geometry causes the length of the C1–C7 bond linking the two rings to increase from its equilibrium value of 2.808 au to 2.824 au, a value that increases further to 2.835 au in the perpendicular geometry.

The delocalization of electrons is determined by the corresponding delocalization of the Fermi hole that governs the spatial extent of the exchange of same-spin electrons.[38] The total exchange of electrons between the basins of the atoms A and B is measured by the delocalization index δ(A,B).[39] The delocalization of the electrons on one ring into the atomic basins of the second ring is indeed found to be maximized for the planar structure; 0.825 electrons or 2.05 % of the electron population of one ring is delocalized onto the other ring in the planar structure. These values decrease to 0.793 e or 1.97 % in the twisted equilibrium geometry and attain their minimum values of 0.723 e or 1.80 % when the two rings are perpendicular. Of the 0.825 e delocalized from one ring onto the other, 0.596 e come from carbon C1 or C7 forming the C–C link between the rings. Thus there is a decrease in delocalization of one-tenth of an electronic charge from one ring onto the other associated with a 0.4 kcal mol^{-1} energy increase in attaining the perpendicular from the planar structure, as determined by the exchange of the electrons between the two rings. The delocalization index between bonded carbons in the same ring, δ(C,C′), varies from 1.3 to 1.4 while the value for δ(C1,C7) equals 1.05 in the planar structure, decreasing to 1.04 in the twisted geometry and attaining its minimum value of 1.00 in the perpendicular geometry.

The rotation causing the formation of the planar structure and the accompanying energy increase of 2.1 kcal mol^{-1} result in a transfer of 0.030 electronic charges from the carbon to the hydrogen atoms. One-half of the charge transfer is from the *ortho*-carbon atoms, that is, those which are linked to the hydrogen atoms that bond to one another in the planar structure, and it is these hydrogens that are the major recipients of the transferred charge, receiving 0.025 e. The major geometric change accompanying the rotation is the increase in the C1–C7 separation by 0.0163 au from the equilibrium value of 2.824 au, a lengthening caused by the accommodation of the approach of the *ortho*-hydrogen atoms. As a consequence, the energies of these two carbon atoms increase by 32.6 kcal mol^{-1}. The energies of the remaining carbon atoms decrease by 9.4 kcal mol^{-1}, the two *para*-carbon atoms accounting for 4.6 kcal mol^{-1} of the decrease. The major decrease in energy in the formation of the planar structure occurs for the H – H bonded hydrogen atoms, the transfer of charge to these hydrogen atoms causing the energy of each to decrease by 5.2 kcal mol^{-1}. The resulting contribution of 20.8 kcal mol^{-1} from the formation of the two H – H bonded interactions accounts for all but 1 kcal mol^{-1} of the energy decrease undergone by all of the hydrogen atoms. The stabilizing energy E(H – H) is thus 10.4 kcal mol^{-1} for each H – H interaction, one that increases to 15.4 kcal mol^{-1} with the 6-31G** basis set in the RHF SCVS calculation and to 15.8 kcal mol^{-1} by using the larger 6-311 ++ G(2d,2p) basis set in a RHF calculation.

The approach of the *ortho*-hydrogen atoms to separations less than the sum of their van der Waals radii upon attaining the planar structure results in H – H bonding and to a stabilizing contribution in excess of 20 kcal mol^{-1} to the energy. The formation of the H – H interactions admittedly causes an increase in the separation between the two rings, one that results in an increase in energy of atoms C1 and C7 linking the rings. There is, however, no "steric nonbonded repulsion" between the *ortho*-hydrogen atoms in the planar structure of biphenyl, just as there is none between the 1,4-hydrogen atoms in molecules **1** and **2**. Instead, the resultant H – H bonding contributes a stabilizing contribution to the energy in all three molecules, one that dominates the accompanying increase in the energy of the carbon atoms in **1** and **2** relative to that of their linear isomers, but is less than the increase in the energies of carbons C1 and C7 in attaining the planar geometry in biphenyl.

Contrasting H – H with dihydrogen bonding

Atomic populations and volumes: A most important characteristic of hydrogen bonding of A–H with B is the transfer of electronic charge from H to both A and B, in the range from 0.01 to 0.1 e,[40, 41] with 0.06 and 0.04 e being transferred from H in forming the ammonia and water dimers, respectively, for example. These transfers increase the already large positive charge on this atom. The hydrogen atoms in the polybenzenoids on the other hand, bear slight negative charges, in the range of a few thousandths of an electronic charge, a charge that increases in magnitude on H – H bonding. Thus the charge of -0.002 e on an *ortho*-hydrogen atom of biphenyl

becomes slightly more negative with $q(H) = -0.008$ e when involved in H – H bonding. Similarly the hydrogen atoms that participate in H – H bonding in **1** and **2** bear charges more negative than the average charge on the remaining hydrogen atoms by -0.004 e in **1** and -0.003 e in **2**. Thus H – H bonding occurs between hydrogen atoms both of which bear small negative charges, and it is accompanied by a small transfer of charge to both hydrogen atoms. The charge redistribution accompanying H – H bonding and its final disposition has no electrostatic component to its energy, making it distinct from the changes involved in hydrogen bonding.

In addition to the H–A length decreasing upon formation of a hydrogen bond, the atomic volume of the hydrogen (v(H)) undergoes a dramatic decrease because of the transfer of electron density to both the A and B atoms and the formation of the H–B interatomic surface.[40, 41] The atomic volume is determined by the intersection of an atom's interatomic surfaces with the 0.001 au density envelope; an envelope that has been shown to yield good agreement with experimentally determined van der Waals radii in the gas phase.[40] The decrease in v(H) for hydrogen is considerable, even for interactions of moderate strength. In the dimers of ammonia and water, for example, the change in v(H) is of the order of 6 au, amounting to a 30% change. There is a much smaller percentage decrease in the volume of the base atom B of $\sim$2.5% for B = N or O.

The volume changes associated with H – H bonding are absolutely and proportionately smaller than for the acidic hydrogen in hydrogen bond formation and occur for both hydrogen atoms. The 0.001 au envelope yields a nonbonded radius of 2.55 au for a benzenoid hydrogen and 2.63 au for a methyl hydrogen. The creation of the H – H interatomic surface in the rotation leading to the attainment of the planar geometry of biphenyl decreases the separation between the *ortho*-protons to within 3.68 au, and the minimum density at their point of contact, the value of ρ_b, is increased to 0.014 au. The rotation causes the volumes of the *ortho*-hydrogen atoms to decrease by 2.5 au from their value of 49.2 au in the twisted equilibrium geometry, a change of 5%. One may determine the effective volume change for the H – H bonded hydrogens in the polybenzenoids by comparing their volumes with the average volume of a hydrogen atom not involved in H – H bonding. This latter volume, equal to 49.7 au, is decreased by 3.2 au or 6% in **1** and by 3.8 au or 8% in **2**.

Atomic energies: The most important difference between H – H and dihydrogen bonding is in the differing energy changes of the involved hydrogen atoms. In hydrogen bonding, the energy of the acidic hydrogen increases and its population and volume decrease. The destabilizing change in energy is considerable, in the range of 20 to 40 kcal mol^{-1} for intermediate to strong interactions.[40, 41] In contrast to this, H – H bonding results in the energy of the pair of atoms being stabilized by amounts up to 10 kcal mol^{-1}.

The decrease in volume coupled with a slight increase in population for the H – H bonded hydrogen atoms means that their average number of electrons per unit volume is greater than for the other hydrogens. This corresponds to a compression of the density of the H – H bonded hydrogen atoms and to an increase in their kinetic energy. For example, the N(H)/v(H) for the *ortho*-hydrogen atoms in biphenyl increases from 0.0207 to 0.0220 e per unit volume in the planar geometry, while the value of T(H)/v(H) increases from 0.0131 au per unit volume to 0.0140 au. The corresponding values for the H – H bonded hydrogens in **1** and **2** exhibit quite similar changes. One might suppose that the compression leads to their destabilization, but this is an erroneous conclusion. It is true that local compressions and expansions in the electron density may be related to corresponding changes in the positive definite form of the kinetic energy *density*, as discussed some time ago,[42] and the *local* statements of the virial theorem provide precise relations between the local kinetic and total energy *densities*.[1] However, for the total molecule bounded at infinity or for one of its constituent atoms bounded by a surface of zero flux, the relations between their average kinetic, potential, and total energies are governed by the virial theorem. In particular for an equilibrium geometry, the virial theorem demands that $E(\Omega) = -T(\Omega)$, in which Ω refers to the *total* molecule or to an atom within the molecule. Thus the compression of the charge distributions of the hydrogen atoms in the formation of an H – H bonded interaction must necessarily lead to an increase in their average electronic kinetic energy, as a consequence of the concomitant lowering in their total energy. Certainly a compression of an atom can lead to an increase in its energy as demonstrated by the quantum definition of pressure in terms of the surface virial of an atom, as illustrated for an $|H_2|$ molecule embedded in an extended chain subject to an applied external pressure.[43] If the compression of the hydrogen atoms resulting from the attainment of the planar geometry in biphenyl, for example, did result in "steric nonbonded repulsions", their kinetic energies would exceed the magnitudes of their total energies by an amount equal to the virial of the external forces acting on their nuclei. Instead, the compression results in a reorganization of the molecular electron density and to a new equilibrium geometry with vanishing forces on all of the nuclei, and the increase in the kinetic energy of the hydrogen atoms results in a stabilizing contribution to the total energy of the planar geometry.

All energy contributions are defined for an open system thus enabling one to determine the origin of the stabilization resulting from H – H bonding.[1] Table 2 gives the kinetic and total energies, together with the attractive and repulsive

Table 2. Contributions to change in energy of *ortho*-hydrogen atoms in the planarization of biphenyl.[a]

	$T(H) = -E(H)$	$V_{neo}(H)$	$V_{net}(H)$	$V_{ee}(H)$	$V_{nn}(H)$	$V_{rep}(H)$	$V(H) = 2E(H)$
equilibrium geometry	0.6520	-1.3332	-16.5792	7.6262	7.6490	15.2752	-1.3040
change in energy	-7.7	-10.5	-173.9	$+78.9$	$+79.5$	$+158.4$	-15.4

[a] Total energies in atomic units, energy differences in kcal mol^{-1}; E(planar) – E(equilibrium). Results are for RHF SCVS 6–31G**//SCVS 6–31G**

contributions to the potential energy, for an *ortho*-hydrogen (*o*-H) atom in the equilibrium geometry of biphenyl, together with the changes in these energies upon attainment of the planar structure and the atom's participation in H–H bonding. The results are for the SCVS calculation, and the energy components and their change with geometry satisfy the requirements of the virial theorem: $T(\mathrm{H}) = -E(\mathrm{H})$ and $E(\mathrm{H}) = (1/2)V(\mathrm{H})$, in which the virial for *o*-H reduces to the potential energy $V(\mathrm{H})$, because of the absence of forces on the nuclei in both geometries. The stabilization energy for a single hydrogen $\Delta E(\mathrm{H}) = -7.7$ kcal mol^{-1} is a result of the decrease in the attractive potential energy (increased stabilization) of the *ortho*-proton, the quantity $\Delta V_{\mathrm{net}}(\mathrm{H})$, exceeding in magnitude the change in the repulsive contributions to the atom's energy, $\Delta V_{\mathrm{rep}}(\mathrm{H})$, the sum of the changes in the electron $V_{\mathrm{ee}}(\mathrm{H})$, and nuclear $V_{\mathrm{nn}}(\mathrm{H})$ energies. The quantity $\Delta V_{\mathrm{net}}(\mathrm{H})$ is the change in the energy of interaction of the *ortho*-proton with the entire electronic charge distribution; the contribution from just the change within the basin of the atom, the quantity $\Delta V_{\mathrm{neo}}(\mathrm{H})$, equals -10.5 kcal mol^{-1}. Thus the repulsive contributions to $\Delta E(\mathrm{H})$ do increase as a result of the *ortho*-hydrogen atoms coming into contact (i.e., sharing an interatomic surface) in the planar geometry, but the resulting redistribution of the density leads to an overriding decrease in the attractive potential energy. Just the opposite behavior is found for the acidic hydrogen upon hydrogen bond formation, with the repulsive energy increase outweighing the decrease in the attractive interactions, as has been previously detailed.[41]

The contribution to the change in energy arising from the formation of an H–H interatomic surface in attaining the planar geometry may be directly determined. This quantity, $V_{\mathrm{s}}(\mathrm{H-H})$, is the virial of the surface forces acting on the H–H interatomic surface.[1, 44] It is obtained by the addition of the surface virials for a bonded pair of *o*-H atoms. The resulting expression for $V_{\mathrm{s}}(\mathrm{H-H})$ is remarkably simple, equaling a force acting through a distance. The force is the one exerted on the electrons in the H–H interatomic surface, $\int \mathrm{d}S\, \sigma(\mathbf{r})$ expressed in terms of the stress tensor $\sigma(\mathbf{r})$, and it is dotted into the distance vector **R** between the two *ortho*-protons. The values of $V_{\mathrm{s}}(\mathrm{H-H})$ are -14.5 and -20.6 kcal mol^{-1} for the DFT and the SCVS calculations, respectively. Both values exceed the corresponding H–H stabilization energies of 10.4 and 15.4 kcal mol^{-1} by approximately 5 kcal mol^{-1}, differences that are accounted for by an increase of $\sim$2.5 kcal mol^{-1} in the value of the C–H surface and basin virials of each hydrogen atom. Similar results are obtained for $V_{\mathrm{s}}(\mathrm{H-H})$ from the H–H surface present in phenanthrene which equals -16.6 kcal mol^{-1} for the SCVS calculation, compared to a stabilization energy of 12.8 kcal mol^{-1}. Thus in each case the formation of the H–H interatomic surface contributes to a decrease in energy by an amount 5 kcal mol^{-1} in excess of the stabilization energy.

Tetra-*tert*-butylindacene (8): There are four H–H bonded interactions linking each of the apical hydrogens on the central benzene to hydrogen atoms on four separate methyl groups in the molecular graph for tetra-*tert*-butylindacene (**8**; Figure 2). Each apical hydrogen thus participates in tetrafurcated H–H bonding and is common to four seven-membered rings, the ring CPs of which are seen in Figure 2. There are no H–H bond paths between the hydrogens within a single *tert*-butyl group, neither in isobutane nor in any of the molecules stabilized by the *tert*-butyl groups. An H–H interaction between a benzenoid hydrogen and a methyl hydrogen in **8** is weaker than one between two benzenoid hydrogens found in the polybenzenoids: it is of greater length and has a lower ρ_{b} value (Table 1).

One may obtain a measure of the extra stability associated with the presence of the H–H bonding in this molecule by performing a rotation of each methyl of the *tert*-butyl groups by 60°, a motion that results in the rupturing of all eight H–H bond paths. The rotation causes the energy to increase by 29 kcal mol^{-1}, part of which arises from the loss of H–H bonding. The same 60° rotation causes the energy of each of the apical hydrogen atoms to increase by 5.6 kcal mol^{-1} and that of each of the four methyl hydrogen atoms bonded to them by 0.5 kcal mol^{-1}. Thus the four H–H bond paths associated with a single apical hydrogen have a total stabilization energy of 7.6 kcal mol^{-1}, and the breaking of the eight H–H bonded interactions on rotation accounts for one-half of the accompanying increase in energy. The apical hydrogen atoms are, therefore, not in repulsive contact with those of the tertiary butyl groups, since a rotation that ruptures the H–H interactions contributes to the resulting increase in energy.

Tetra-*tert*-butyltetrahedrane (6) and tetra-*tert*-butylcyclobutadiene (7): Balci, McKee, and Schleyer[34] have determined the equilibrium structures of molecules **6** and **7** using RHF and B3LYP of density functional theory with the 6-31G* basis set. The ring in **7** is predicted to have unequal bond lengths of 1.354 and 1.608 Å, leading to a lowest energy structure of C_2 symmetry, in agreement with the most recent X-ray structure of this compound and other twisted cyclobutadiene derivatives. The unequal bond lengths are reflected in the different delocalization values $\delta(\mathrm{C,C'})$, the long bond yielding a value of 0.92 and the short one a value of 1.73. Tetra-*tert*-butyltetrahedrane (**6**) is found to have a minimum energy structure of T symmetry, one which is 0.5 kcal mol^{-1} lower in energy than the more symmetrical T_d structure. Our B3LYP calculations using the 6-31G** and 6-311++G(2d,2p) basis sets at the 6-31G* geometries of Balci et al. yield an excess stability of the T over the T_d structure of 0.8 and 0.6 kcal mol^{-1}, respectively.

In their discussion of **6**, Balci et al. note that: "In the T_d symmetry structure there are 12 nonbonded H$\cdots$H interactions of 2.25 Å which are reduced to 12 H$\cdots$H interactions of 2.43 Å in the T-symmetry structure." There are indeed 12 equivalent H–H bond paths for H–H separations of 4.25 au in the T_d structure that are transformed into 12 longer H–H bond paths for H–H separations of 4.59 au in the T structure. However, another six still longer H–H bond paths are present in the T structure with H–H separations of 5.13 au (Table 1 and Figure 2). Thus the 12 H–H bonded interactions in the T_d structure with $\rho_{\mathrm{b}} = 0.0065$ au are replaced by 18 interactions in the T structure with ρ_{b} values of 0.0048 and 0.0028 au, respectively, the larger basis set giving

values that differ by no more than 0.0001 au. Of the three hydrogen atoms of a methyl group in the T_d structure, one is normal and each of the remaining two is H – H bonded to a methyl on a neighboring *tert*-butyl group. Thus each methyl group is linked to two methyls of other *tert*-butyl groups. Of the three hydrogen atoms of a single methyl group in the T structure, one is normal and another is engaged in bifurcated H – H bonding, being linked to a corresponding bifurcated hydrogen atom on a methyl ($\rho_b = 0.0028$ au) and to a hydrogen atom in another methyl group ($\rho_b = 0.0048$ au), both methyls being on a neighboring *tert*-butyl group (Figure 2). Thus each methyl group in the T structure is linked to three other methyl groups on two other *tert*-butyl groups.

The energy analysis is given in terms of the results from the large basis set. Each H – H interaction in the T_d structure has a stabilization energy of 1.6 kcal mol^{-1}. The energy of a hydrogen atom engaged in bifurcated H – H bonding in the T structure has a stabilization energy of 1.1 kcal mol^{-1}, while the energy of the singly bonded hydrogen atom is the same as that of a normal hydrogen atom to within the integration error of less that 0.1 kcal mol^{-1}. Thus the 12 H – H interactions contribute 19.2 kcal mol^{-1} to the stabilization of the T_d structure and the 18 such interactions contribute 13.2 kcal mol^{-1}, or $\sim$0.8 kcal mol^{-1} per H – H interaction, to the T structure leading to a *reduction* in the stabilizing contribution from H – H bonding in passage from the T_d to the more stable T structure.

Balci et al. state: "The driving force behind the ($T_d \rightarrow T$) distortion is the relief of steric repulsion between methyl groups on different *tert*-butyl groups." They also employ group additivity increments, free from *exo*-substituent interactions, to compute a heat of formation for tetra-*tert*-butyl tetrahedrane that is 15.3 kcal mol^{-1} higher than a computed heat of formation, an energy that they attribute to steric repulsion between the *tert*-butyl groups. These classical strain arguments are made in the absence of knowledge of the H – H stabilizing interactions that are present in both the T and T_d structures and of the changes in energies of the individual atoms and groups accompanying the $T_d \rightarrow T$ transformation, an analysis that clarifies the role of the H – H stabilization energies. It should be recalled that the energies, and indeed all properties, determined within the theory of atoms in molecules recover experimental group additivity schemes and do so in a manner that makes the additive behavior both understandable and predictable.[1, 45] For example, a methyl group in normal hydrocarbons past propane exhibits perfect transferability (within both experimental and theoretical accuracy) in its charge distribution and hence properties. It necessarily differs slightly from a methyl group in ethane that is electrically neutral. In bonding to a methylene group, not only is charge conserved—the electronic charge gained by methyl of ethane equaling that lost by methylene—but energy is similarly conserved. Thus incremental group additivity is maintained in spite of intergroup charge transfer by the process of *compensatory transferability*, a process of not uncommon occurrence in view of Benson's extensive tabulation of incremental group properties.[46] In a process where compensatory transferability does not apply and the group increments do not account for a change in energy, one may employ the atomic energies of QTAIM to isolate the cause of the difference. The energy of a CH_2 in cyclopropane, for example,[1] is found to exceed the transferable energy of the same group in a linear hydrocarbon by one-third of the classical strain energy assigned to the cyclic molecule, a consequence of a transfer of density from H to C.

Changes in geometrical parameters accompanying the $T_d \rightarrow T$ transformation must necessarily lead to changes in the electron density distribution, since the density determines the Hellmann – Feynman forces acting on the nuclei. The principal geometrical changes for $T_d \rightarrow T$ are a shortening of the lengths of the C–C bonds in the C_4 cage by 0.0014 Å and of the bonds between a cage C atom and the C atom of a *tert*-butyl group by 0.0020 Å. The remaining bond lengths all increase, but by amounts less than 0.0004 Å. Since all bonds linking a cage carbon atom shorten in $T_d \rightarrow T$, it is not surprising that these carbon atoms undergo the largest individual changes in energy, being stabilized by 3.0 kcal mol^{-1}, and in population, which increases by 0.0004 e. The cage carbon atoms thus make the largest contribution to the increase in stability of the T structure, a contribution of -12.1 kcal mol^{-1}. Each unique carbon atom of a *tert*-butyl group, in addition to the shortening of its links to the cage, also undergoes a lengthening of its bonds with its three bonded methyl groups, and the contribution of all four such carbon atoms is a net destabilization of the T structure by $+2.9$ kcal mol^{-1}. Because of the bond lengthening and a concomitant loss of 0.009 e of electronic charge, the 12 carbon atoms of the methyl groups are destabilized in the T structure and contribute $+13.1$ kcal mol^{-1} to $T_d \rightarrow T$. In total, the hydrogens are more stable in T than in T_d and contribute -4.8 kcal mol^{-1} to the energy change. Thus overall, the methyl groups are *destabilized* by 8.3 kcal mol^{-1} in the $T_d \rightarrow T$ transformation. Consequently, the stabilization of the T over the T_d structure is not a result of a decrease in the repulsion between the *tert*-butyl groups. Instead, the methyl groups are actually destabilized in the $T_d \rightarrow T$ transformation, and the overriding energy change comes from the stabilizing re-organization of the electron density in the interior of the molecule—of the carbon atoms in the tetrahedral cage. The 6-31G** results yield the same analysis of the $T_d \rightarrow T$ transformation.

There are a total of 12 H – H bonded interactions in tetra-*tert*-butylcyclobutadiene (**7**), grouped into two sets. Two hydrogens of one methyl on one isobutyl group are each H – H bonded to hydrogen atoms on methyl groups linked to two other isobutyl groups. These latter hydrogen atoms are in turn engaged in bifurcated H – H bonding, as pictured in Figure 2. Three of the H – H interactions between two bifurcated hydrogens have ρ_b values of 0.0168 au, the remaining three have values of 0.0152 au. The six H – H interactions between a bifurcated and a singly H – H bonded atom also fall into two groups, one set with ρ_b values of 0.0080 au, the other with values of 0.0068 au. In this manner there are six H – H bonded interactions linking the three methyls of one isobutyl group with two of the methyls on two neighboring isobutyl groups, and another set of six interactions linking these methyl groups with the methyl groups on the fourth isobutyl group.

The six H – H bonded interactions between hydrogen atoms engaged in bifurcated bonding in **7** are shorter and possess larger ρ_b values than the shortest and strongest of the H – H interactions is found in the T_d structure of **6**. Thus it is not surprising that the bifurcated hydrogens in **7** exhibit a considerable increase in stability over the normal hydrogens, equaling 6.5 kcal mol^{-1}. The remaining hydrogens involved in H – H bonding are stabilized by 0.4 kcal mol^{-1}, and the stabilization energy resulting from the H – H interactions in **7** is 55.2 kcal mol^{-1} compared to the 19.2 and 13.2 kcal mol^{-1} for the T_d and T structures of **6**. Thus the tighter "corset"[26] enclosing the cylcobutadiene ring leads not to greater nonbonded repulsions, but to a greater stabilization energy than does the looser corset enclosing the tetrahedral cage in **6**.

Heating is known to cause **6** to isomerize to **7**. The calculations reported by Balci et al., including estimates of heats of formation at both 0 and 298 K, predict nearly equal stabilities for both molecules, with **6** more stable than **7** by approximately 1.5 kcal mol^{-1}; the present B3LYP/6-31G** calculation yields an energy difference of 1.2 kcal mol^{-1}. The closer approach of the methyl hydrogen atoms in **7** compared to **6**, with the concomitant increase in the H – H stabilization energy, indicates the driving force for the thermal isomerization of **6** to **7** to be the increased stability of the methyl groups in **7**. The methyl groups in **7** are more stable than those in **6** by 125 kcal mol^{-1}. The energies of the four cage carbon atoms increase by 158 kcal mol^{-1} in forming the cyclobutadiene ring, the four isobutyl carbon atoms accounting for the remaining 32 kcal mol^{-1} decrease in energy. Thus the overriding energy change accompanying the transformation of **6** to **7** is an increase in stability of the methyl groups that is partially (in reality) or completely (by present calculations) counteracted by a decrease in the stabilities of the carbon atoms of the cage.

Conclusion

The atomic interaction line resulting when a bonded hydrogen atom is pushed against another atom in a closed-shell interaction does not necessarily result in a "nonbonded repulsion" and an increase in energy. If the hydrogen is acidic and the other atom basic, the atomic interaction line is a bond path characterizing hydrogen bonding. If both atoms are hydrogen and possess disparate charges, the resulting bond path indicates the presence of "dihydrogen bonding", an interaction similar in all respects to hydrogen bonding. If a hydrogen atom bearing a slight negative charge is placed in close proximity to a transition metal atom, the result is not a repulsion, but rather the formation of a bond path that signifies the presence of an agostic interaction, one whose characteristics are distinct from those of hydrogen bonding.[47] The presence of a bond path linking a titanium atom to a methyl hydrogen has been demonstrated in both experimental and theoretical charge distributions.[47,48]To this list one may now add "H – H bonding", a bonded interaction resulting from the close approach of two bonded hydrogen atoms bearing the same or similar net charges. While also a closed-shell interaction, H – H bonding is distinct from hydrogen bonding in its atomic and geometric characteristics. One anticipates, however, that just as hydrogen bonding exhibits characteristics that range from closed-shell to shared interactions as the strength of the interaction increases,[10, 40, 49] so H – H bonding may be found to merge with dihydrogen bonding, as the disparity in the charges on the two participating hydrogens increases.

The classification of H – H interactions as "nonbonded steric repulsions" in molecules such as the benzenoid hydrocarbons is at variance with the demonstrated stabilizing contribution their presence makes to the molecular energy. Such interactions must in fact be ubiquitous, their stabilization energies contributing to the sublimation energies of hydrocarbon molecular crystals and accounting for the existence of solid hydrogen. The intermolecular H – H bonding in solid hydrogen, modeled by a linear chain of molecules, has been documented and its variation with pressures up to 160 GPa determined.[43] At low pressures the intermolecular H – H bonding exhibits the closed-shell characteristics described here, but with increasing pressure and the resulting accumulation of density in the intermolecular regions, the H – H interactions increasingly assume the characteristics of a shared interaction. This is accompanied by an increasing delocalization of the density—a process that eventually culminates in the equal delocalization of the density over a set of equally spaced atoms in the atomic metallic state.

H – H bonding falls in the class of "van der Waals" interactions operative in all molecular crystals, no different in kind, for example, from the intermolecular Cl – Cl bonding present in solid chlorine.[8] The ability to identify specific interactions within a crystal, as defined in terms of the associated bond paths and determine their directional and atomic characteristics, aids in quantifying our understanding of the cohesive properties of molecular crystals.[4]

Acknowledgement

We wish to thank Dr. Fernando Cortes for his comments on this manuscript and for his assistance in its preparation.

Note added in proof: In a personal communication, Professor T. Stanley Cameron, Professor Osvald Knop, and Dr. Katherine Robertson (all of the Department of Chemistry, Dalhousie University, Halifax, Nova Scotia, Canada) kindly informed us of their observation of intermolecular H – H bond paths between hydrogen atoms of neighboring phenyl groups in experimental density distributions of salts of tetraphenylborates.

[1] R. F. W. Bader, *Atoms in Molecules: A Quantum Theory*, Oxford University Press, Oxford (UK), **1990**.
[2] R. F. W. Bader, S. G. Anderson, A. J. Duke, *J. Am. Chem. Soc.* **1979**, *101*, 389 – 1395.
[3] W. Bader, Y. Tal, S. G. Anderson, T. T. Nguyen-Dang, *Isr. J. Chem.* **1980**, *19*, 2871 – 2883.
[4] T. S. Koritsanszky, P. Coppens, *Chem. Rev.* **2001**, *101*, 1583 – 1628.
[5] A. Keith, R. F. W. Bader, Y. Aray, *Int. J. Quantum Chem.* **1996**, *57*, 183 – 198.
[6] F. W. Bader, *Phys. Rev. B* **1994**, *49*, 13348 – 13356.
[7] F. W. Bader, *J. Phys. Chem. A* **1998**, *102*, 7314 – 7323.
[8] V. Tsirelson, P. F. Zou, T.-H. Tang, R. F. W. Bader, *Acta Crystallogr. Sect. A.* **1995**, *51*, 143 – 153.
[9] R. Flaig, T. Koritsanszky, B. Dittrich, A. Wagner, P. Luger, *J. Am. Chem. Soc.* **2002**, *124*, 3407 – 3417.

[10] E. Espinosa, E. Molins, C. Lecomte, *Chem. Phys. Lett.* **1998**, *285*, 170 – 173.
[11] P. L. A. Popelier, F. M. Aicken, S. E. O'Brien, *Atoms in Molecules, Vol. 1*, The Royal Society of Chemistry, Cambridge (UK), **2000**, pp. 143 – 198.
[12] P. L. A. Popelier, P. J. Smith, *Quantum Topological Atoms*, *Vol. 2*, The Royal Society of Chemistry, Cambridge (UK), **2002**, pp. 391 – 448.
[13] Y. A. Abramov, L. Brammer, W. T. Klooster, R. M. Bullock, *Inorg. Chem.* **1998**, *37*, 6317.
[14] J. Cioslowski, S. T. Mixon, *Can. J. Chem.* **1992**, *70*, 443 – 449.
[15] R. Custelcean, J. E. Jackson, *Chem. Rev.* **2001**, *101*, 1963 – 1980.
[16] T. B. Richardson, S. de Gala, R. H. Crabtree, P. E. M. Siegbahn, *J. Am. Chem. Soc.* **1995**, *117*, 12875 – 12876.
[17] P. L. A. Popelier, *J. Phys. Chem. A* **1998**, *102*, 1873 – 1878.
[18] S. J. Grabowski, *J. Phys. Chem. A* **2001**, *105*, 10739 – 10746.
[19] S. J. Grabowski, *J. Mol. Struct.* **2000**, *553*, 151 – 156.
[20] S. J. Grabowski, *J. Phys. Chem. A* **2000**, *104*, 5551 – 5557.
[21] S. J. Grabowski, *Chem. Phys. Lett.* **2000**, *327*, 203 – 208.
[22] S. A. Kulkarni, A. K. Srivastava, *J. Phys. Chem. A* **1999**, *103*, 2836 – 2842.
[23] C. F. Matta, R. F. W. Bader, *Proteins: Struct. Funct. Genet.* **2000**, *40*, 310 – 29.
[24] I. Alkorta, J. Elguero, O. Mó, M. Yáñez, J. E. Del Bene, *J. Phys. Chem. A* **2002**, *106*, 9325 – 9330.
[25] R. F. W. Bader, *Can. J. Chem.* **1998**, *76*, 973 – 988.
[26] G. Maier, *Angew. Chem.* **1988**, *100*, 317 – 341; *Angew. Chem. Int. Ed. Engl.* **1988**, *27*, 309 – 332.
[27] G. Maier, S. Pfriem, *Angew. Chem.* **1978**, *90*, 551 – 552; *Angew. Chem. Int. Ed. Engl.* **1978**, *17*, 519 – 520.
[28] J. D. Dunitz, C. Krüger, H. Irngartiner, E. F. Maverick, Y. Wang, M. Nixdorf, *Angew. Chem.* **1988**, *100*, 415 – 418; *Angew. Chem. Int. Ed. Engl.* **1988**, *27*, 387 – 389.
[29] C.-C. Wang, T.-H. Tang, L. Chen, Y. Wang, personal communication **2002**.
[30] Gaussian 94 (Revision B.2), M. J. Frisch, G. W. Trucks, H. B. Schlegel, P. M. W. Gill, B. G. Johnson, M. A. Robb, J. R, Cheeseman, T. Keith, G. A. Petersson, J. A. Montgomery, K. Raghavachari, M. A. Al-Laham, V. G. Zakrzewski, J. V. Ortiz, J. B. Foresman, J. Cioslowski, A. Nanavakkara, M. Challacombe, C. Y. Peng, P. Y. Ayala, W. Chen, M. W. Wong, J. L. Andres, E. S. Replogle, R. Gomperts, R. L. Martin, D. J. Fox, J. S. Binkley, D. J. Defrees, J. Baker, J. P. Stewart, M. Head-Gordon, C. Gonzalez, J. A. Pople, Gaussian, Inc., Pittsburgh, PA, **1995**.
[31] F. W. Biegler-König, R. F. W. Bader, T.-H. Tang, *J. Computer Chem.* **1982**, *13*, 317 – 328.
[32] F. Biegler-König, J. Schönbohm, *J. Computer Chem.* **2002**, *23*, 1489 – 1494.
[33] F. W. Biegler-Konig, J. Schönbohm, D. Bayles, *J. Computer Chem.* **2001**, *22*, 545 – 559.
[34] M. Balci, M. L. McKee, P. von R. Schleyer, *J. Phys. Chem. A* **2000**, *104*, 1246 – 1255.
[35] R. G. A. Bone, R. F. W. Bader, *J. Phys. Chem. A* **1996**, *100*,10892 – 10911.
[36] *CRC Handbook of Chemistry and Physics, 81st Edition*, CRC Press, New York, NY, **2000**.
[37] A. Almenningen, O. Bastiansen, L. Fernholt, B. N. Cyvin, S. J. Cyvin, S. Samdal, *J. Mol. Struct.* **1985**, *128*, 59 – 76.
[38] R. F. W. Bader, M. E. Stephens, *J. Am. Chem. Soc.* **1975**, *97*, 7391 – 7399.
[39] X. Fradera, M. A. Austen, R. F. W. Bader, *J. Phys. Chem. A* **1999**, *103*, 304 – 314.
[40] R. F. W. Bader, M. T. Carroll, J. R. Cheeseman, C. Chang, *J. Am. Chem. Soc.* **1987**, *109*, 7968 – 7979.
[41] M. T. Carroll, R. F. W. Bader, *Mol. Phys.* **1988**, *65*, 695 – 722.
[42] R. F. W. Bader, H. J. T. Preston, *Int. J. Quantum Chem.* **1969**, *3*, 327 – 347.
[43] R. F. W. Bader, M. A. Austen, *J. Chem. Phys.* **1997**, *107*, 4271 – 4285.
[44] J. Hernández-Trujillo, R. F. W. Bader, *J. Phys. Chem. A* **2000**, *104*, 1779 – 1794.
[45] R. F. W. Bader, P. L. A. Popelier, T. A. Keith, *Angew. Chem.* **1994**, *106*, 647 – 658; *Angew. Chem. Int. Ed. Engl.* **1994**, *106*, 620 – 631.
[46] S. W. Benson, F. R. Cruickshank, D. M. Golden, G. R. Haugen, H. E. O'Neal, A. S. Rodgers, R. Shaw, R. Walsh, *Chem. Rev.* **1969**, *69*, 279.
[47] P. L. A. Popelier, G. Logothetis, *J. Organomet. Chem.* **1998**, *555*, 101 – 111.
[48] W. Scherer, W. Hieringer, M. Spiegler, P. Sirsch, G. S. McGrady, A. J. Downs, A. Haaland, B. Pedersen, *Chem. Commun.* **1998**, 2471 – 2472.
[49] C. Flensburg, S. Larsen, R. F. Stewart, *J. Phys. Chem.* **1995**, *99*, 10130 – 10141.

Received: November 29, 2002 [F4626]

